International Journal of Environmental Science and Technology
https://doi.org/10.1007/s13762-021-03822-0

ORIGINAL PAPER

Insights into the generation of hydroxyl radicals from H_2O_2 decomposition by the combination of Fe^{2+} and chloranilic acid

M. I. Ahmad[1] · N. Bensalah[2]

Received: 18 December 2020 / Revised: 19 August 2021 / Accepted: 17 November 2021
© The Author(s) 2021

Abstract

In this work, the degradation of chloranilic acid (CAA) by chemical oxidation with H_2O_2 alone and in the presence of ferrous iron Fe^{2+} catalyst was investigated in order to improve our understanding on the novel metal-independent approach. The interesting and efficient metal-independent hydroxyl radicals (OH) production by using halogenated quinones and H_2O_2 has been currently demonstrated. The results clearly confirmed the formation of OH radicals from the reaction of CAA with H_2O_2. CAA was slowly decayed by chemical oxidation with H_2O_2 and followed a pseudo-first kinetics. H_2O_2 doses ≥ 1000 mM were required to achieve complete CAA decay from 1 mM CAA. However, low total organic carbon (TOC) removal was measured with the accumulation of carboxylic acids. The addition of Fe^{2+} enhanced the kinetics of CAA degradation and reduced the required dose of H_2O_2. High TOC removal was obtained, almost complete release of chloride ions, without accumulation of carboxylic acids. The decolorization of methylene blue (MB) aqueous solutions was performed using H_2O_2, H_2O_2/CAA, H_2O_2/Fe^{2+}, and H_2O_2/CAA/Fe^{2+}. H_2O_2/CAA/Fe^{2+} was the most effective method in decolorizing MB solutions due to the accelerated Fe^{2+} regeneration. Coupling Fenton reagent with CAA seems to be promising alternative to physical activation in water and soil treatment.

Keywords Hydrogen peroxide · Chloranilic acid · Chemical oxidation · Fenton reagent · Hydroxyl radicals

Introduction

Historically, Fenton reaction is based on the production of hydroxyl radicals by catalytic decomposition of hydrogen peroxide (H_2O_2) using a transition metal, mainly Fe^{2+}, as a catalyst (Eq. 1) (Babuponnusami and Muthukumar 2014; Pliego et al. 2015; M. hui Zhang et al. 2019; Oturan et al. 2012; Oliveira et al. 2014).

$$H_2O_2(aq) + Fe^{2+}(aq) \rightarrow Fe^{3+}(aq) + {}^{\cdot}OH(aq) + HO^{-}(aq) \quad (1)$$

This reaction was recognized by its great success and high efficiency to remove many organic and inorganic recalcitrant compounds from soil and water (Telles and Granhen Tavares 2012; Nidheesh et al. 2013; Yue et al. 2015; Martínez-Costa et al. 2018; Giraldo-Aguirre et al. 2018; Verma and Chaudhari 2020). This is due to the intensive oxidative power, short lifetime, and high reactivity of the ${}^{\cdot}OH$ radicals (Cheng et al. 2016; Buxton et al. 1988; García et al. 2013). These unique characteristics enable them to immediately react with the pollutant molecules in a non-selective way (Gligorovski et al. 2015; Keen et al. 2014). Generally, the degradation of pollutants by Fenton's reagent ended with their transformation into harmless substances that pause little environmental concerns.

Nevertheless, this reaction is thermodynamically feasible at any pH; however, it is kinetically possible only at pH in the range 2–3 (Duesterberg et al. 2008; Jeong et al. 2010). This is limiting the utilization of Fenton process for the treatment to only acid streams. In addition, the slowness of the regeneration of the catalyst Fe^{2+} (rate-determining step (Eqs. 2–3)) requires the addition of high amounts of Fe^{2+} to

Editorial responsibility: Anna Grobelak.

✉ N. Bensalah
nasr.bensalah@qu.edu.qa

[1] Central Laboratories Unit (CLU), Qatar University, PO Box 2713, Doha, Qatar

[2] Program of Chemistry, Department of Chemistry and Earth Sciences (DCES), College of Arts and Sciences, Qatar University, PO Box 2713, Doha, Qatar

Published online: 03 December 2021

accelerate the degradation of pollutants by continuous feed up of $^{\cdot}OH$ radicals (Li et al. 2019; Qiang et al. 2003).

$$Fe^{3+}(aq) + H_2O_2(aq) \rightarrow Fe^{2+}(aq) + HO_2^{\cdot} + H^+(aq) \quad (2)$$

$$Fe^{3+}(aq) + HO_2^{\cdot} \rightarrow Fe^{2+}(aq) + O_2 + H^+(aq) \quad (3)$$

Furthermore, post-treatment including chemical reduction, acid–base reaction, and filtration is often needed to remove the excess of oxidant H_2O_2, neutralize the treated water, and remove the iron(III) hydroxide ($Fe(OH)_3$) precipitate (Eq. 4) (Chen et al. 2011; Boonrattanakij et al. 2011). This post-treatment adds unnecessary costs to the whole treatment process.

$$Fe^{3+}(aq) + 3OH^-(aq) \rightarrow Fe(OH)_3(s) \downarrow \quad (4)$$

Several attempts have been made to improve the performance of Fenton reaction in the treatment of natural waters and wastewaters (Babuponnusami and Muthukumar 2014; Pliego et al. 2015; M. hui Zhang et al. 2019; Thomas and Zdebik 2019; Thomas et al. 2017). The replacement of homogeneous Fe^{2+} catalyst with natural and synthetic heterogeneous catalysts reduced the costs of the process due to the possibility of recycling of the catalysts; however, it inhibited the pollutants degradation (Nidheesh 2015; Rahim Pouran et al. 2014). Combining Fenton with UV irradiation (known as photo-Fenton process) promoted the efficiency of pollutants degradation, enhanced the regeneration of the catalyst, and reduced its quantity (Ameta et al. 2018; Clarizia et al. 2017). Improved efficiency has been achieved with electro-Fenton, photo-electro-Fenton, and sono-electro-Fenton processes (Liu et al. 2018; Ganiyu et al. 2018).

On the other hand, Chen et al. (Chen and Pignatello 1997) demonstrated the important role played by quinone intermediates as electron shuttles in Fenton and photo-Fenton oxidations of phenol derivatives. It was validated through experimental and simulation investigations that quinone intermediates transfer electrons to Fe^{3+}, which facilitates the oxidation of the target compound. The conversion of quinone into semiquinone is complemented with the reduction of Fe^{3+} into Fe^{2+}, thus accelerating the catalytic cycle of iron in the whole Fenton oxidation. Duesterberg and Waite (Duesterberg and Waite 2007) confirmed the results obtained by Chen et al. (Chen and Pignatello 1997) related to the role of quinones in the redox cycling of iron in Fenton process. These results implicated that the addition of co-oxidants such as quinones would solve the problems related to regeneration of Fe^{2+} catalyst in Fenton oxidation mechanisms, which reduces the required amounts of Fe^{2+}, and thus that of the solid wastes. Furthermore, Zhu et al. (Zhu et al. 2002, 2012) demonstrated the metal-independent production of hydroxyl radicals from the reaction between hydrogen peroxide and tetrachloro-1,4-benzoquinone. Recently, Li et al. (Li et al. 2013) proved theoretically the possible production of OH radicals by the reaction between halogenated benzoquinone derivatives and hydrogen peroxide (H_2O_2) (Fig. 1).

This work aims to improve our understanding on the novel metal-independent approach and Fe^{2+}-catalyzed H_2O_2 decomposition and the combined system for the production of OH radicals and their application for removing organic pollutants in water. The efficiency of using quinone derivatives in producing in situ hydroxyl radicals by reaction with hydrogen peroxide in the absence of Fe2 + catalyst will be also demonstrated. The effect of addition of quinone derivatives on efficiency of Fenton reaction in

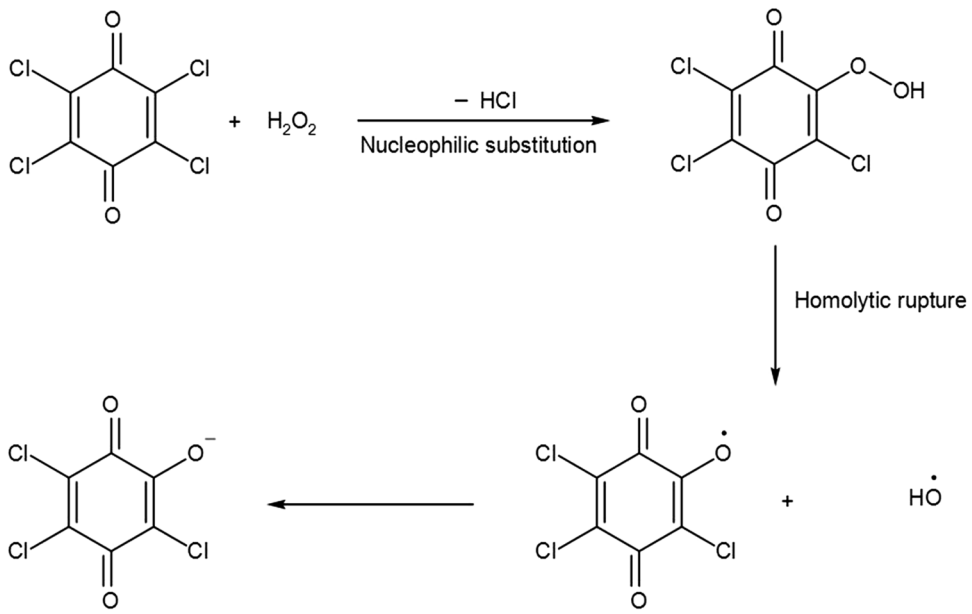

Fig. 1 Mechanism of production of OH radicals by nucleophilic attack of H_2O_2 onto tetrachloro-1,4-benzoquinone (Zhu et al. 2007)

decolorizing methylene blue solutions will be also evaluated. These findings will be important to explore and expand the implementation of H_2O_2-based methods in water treatment plants. Chloranilic acid (2,5-dichloro-3,6-dihydroxybenzoquinone), CAA, was selected as quinone derivative to be reacted with H_2O_2. In the first part of this work, the degradation of CAA by H_2O_2 alone (to confirm the production of hydroxyl radicals by inter) and in the presence of ferrous iron Fe^{2+} catalyst was investigated. In fact, CAA was detected among others as stable halo-benzoquinone disinfection by-products in treated water (Wang et al. 2014, 2016). It has been detected in pulp mill bleaching effluents and polychlorophenols industrial wastewaters (Treviño-Quintanilla et al. 2011; Martínez-Huitle et al. 2004; Zhu et al. 2010). In the second part, the degradation of methylene blue dye was assessed by H_2O_2/CAA, H_2O_2/Fe^{2+}, H_2O_2/CAA/Fe^{2+} systems. The experimental work was carried out at Central Lab Unit at Qatar University (October 2019-March 2020).

Materials and methods

Chemicals

Chloranilic acid (2,5-Dichloro-3,6-dihydroxy-benzoquinone) was received from Fluka (analytical grade, > 99%) and was used without further purification. Phenol, benzoic acid, and hydroquinone were bought from Sigma-Aldrich (> 99%). Hydrogen peroxide (30% H_2O_2 by mass) and ethanol (C_2H_5OH, > 99%) were VWR chemicals. Iron(II) sulfate hepta hydrate ($FeSO_4$. $7H_2O$), sodium hydroxide (NaOH), sodium sulfite (Na_2SO_3), and sulfuric acid (H_2SO_4) were analytical grade Sigma-Aldrich chemicals. Deionized water received from Millipore Milli-Q equipment with resistivity ≥ 18.2 MΩ.cm and TOC content ≤ 5 ppb was used to prepare the aqueous solutions.

Experimental procedures

The degradation experiments were carried out in a 500-mL double-jacket glass reactor equipped with a magnetic stirrer and a thermometer. The temperature was maintained to room temperature (23–25 °C) by water circulation. The pH of 250 mL CAA (or MB) aqueous solution was adjusted to the desired value by addition of drops of 0.1 M NaOH or H_2SO_4. A precise amount hydrogen peroxide 30% was added to 250 mL of the solution to be treated. In Fenton experiments, an aliquot of 1000 mM Fe^{2+} aqueous solution was mixed with the CAA/MB aqueous solution before H_2O_2 is added. In all experiments, the degradation starts when H_2O_2 is added. All the experiments were performed in duplicate. 5 mL samples were periodically collected and immediately quenched with Na_2SO_3 or ethanol. All the samples withdrawn at desired times underwent a filtration through 0.2-µm membrane filters before analysis (three measurements for each sample).

Analytical methods

TOC analysis was conducted using a Skalar Formacs^{HT} TOC/TN analyzer. UV–visible spectrophotometer (Perkin Elmer Lambda 5) was used for UV–visible spectra plotting using a 1-cm quartz cells. The pH was monitored using a pH-meter (Seven Compact S210, METTLER TOLEDO®). The analysis of chloride ions was performed by ion chromatograph (Dionex ICS 2000) using Ion Pac AS 19 column. DS6 conductometric cell was used as detector in parallel with ASRS 300 mm-4 mm suppressor. The limit of detection (LOD) of this method for chlorides was 0.025 mg/L. CAA concentrations were measured using HPLC using Shimadzu 20A Gradient LC System with UV–Vis Detector equipped with Shim-pack GWS C18 (150 × 4.6, 5 µm) column. A mixture of solvent A (1% CH_3CO_2H aqueous solution) and solvent B (methanol, CH_3OH) was used as mobile phase with 1 mL/min flow rate. The temperature of the separation column was maintained at 30 °C during the analysis. The injection volume was fixed to 10 µL for all samples. Gradient elution mode was used as follows: 100% solvent A is eluted for 1 min, then the elution gradient of solvent B is linearly increased to reach 100% after 25 min, and finally 100% solvent B is eluted for 8 min. The wavelength of the UV detector was fixed at 248 nm. In these conditions, LOD for CAA was estimated to be 0.08 mg/L with 101% recovery. The same chromatograph was used to analyze phenol, benzoic, acid, and hydroquinone. The mobile phase is composed of a mixture of eluent C (0.1% HCO_2H in H_2O) and eluent D (0.1% HCO_2H in CH_3CN). The analysis of oxalic and maleic acids was performed using HPLC instrument equipped with Supelcogel H column. The mobile phase consists of 0.15% H_3PO_4 aqueous solution with a constant flow rate of 0.15 mL/min. The UV detector was set a wavelength of 210 nm. External standardization method was used for all the analytes in chromatography analysis (linear curves with regression coefficient $r^2 > 0.99$).

Results and discussion

Degradation of CAA by chemical oxidation with H_2O_2

Figure 2 presents the effect of H_2O_2 dose on the changes of CAA concentration with time during the chemical oxidation of CAA (1 mM) by H_2O_2 in aqueous solution holding the other operating conditions unchanged (initial pH = 3.0, T = 23–25 °C, stirring: 300 rpm). The degradation of CAA

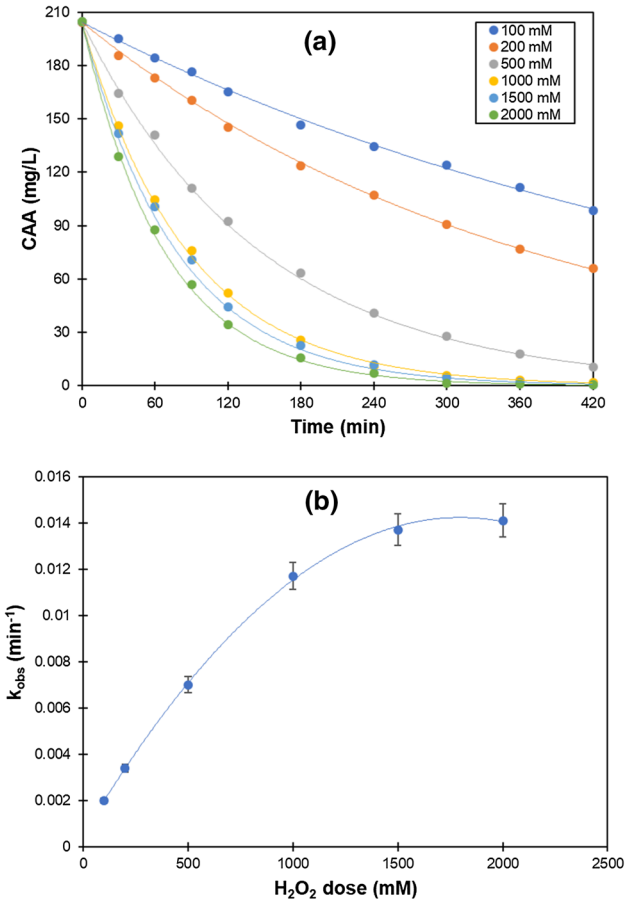

Fig. 2 Chemical oxidation of CAA by H_2O_2: effect of H_2O_2 dose **a** degradation of CAA, **b** pseudo-first-order rate constant k_{obs}. Operational conditions: initial CAA concentration: 209 mg/L (1 mM), H_2O_2 dose: 100–2000 mM, initial pH = 3.0, T = 23–25 °C, stirring rate: 300 rpm

was performed at pH = 3.0 to keep same pH conditions than Fenton reaction for sake of comparison. As it can be seen from Fig. 2.a, CAA concentration decreased with time for H_2O_2 doses in the range 100–2000 mM (the stoichiometric amount of H_2O_2, 1 mM, showed an observable change in CAA concentration after 24 h). The increase in H_2O_2 dose enhanced the rate and the yield of CAA depletion. CAA depletion yield (calculated after 420 min) increased from 51.7% at 100 mM H_2O_2 to 67.8, 92.2, 99.1, 99.6, 99.9% at 200, 500, 1000, 1500, and 2000 mM H_2O_2, respectively. In addition, the graphs of CAA with time had an exponential trend for H_2O_2 doses indicating that the chemical oxidation of CAA by H_2O_2 follows a pseudo-first-order kinetics with rate constant k_{obs}. Thus, the rate law can be given by the equation:

$$r = -\frac{d[CAA]}{dt} = k_{obs}[CAA] \quad (5)$$

Figure 2b shows that the rate constant k_{obs} increases linearly with H_2O_2 concentration up to 1000 mM, and then it becomes slightly affected by H_2O_2 concentration for higher concentrations than 1000 mM. The results indicated that H_2O_2 is capable of removing CAA from aqueous solutions under normal conditions of pH and temperature. An aqueous solution containing 1 mM CAA required 1000 mM H_2O_2 to achieve almost complete depletion of CAA within 420 min. Higher H_2O_2 doses than 1000 mM did not have a significant enhancement in the rate of the reaction. These results are in good agreement with those reported in the literature related to the chemical oxidation of halogenated semi-quinones with hydrogen peroxide (Zhu et al. 2002, 2012, 2007; Li et al. 2013). Similarly, the chemical oxidation of CAA by H_2O_2 would involve a nucleophilic substitution of Cl by OOH followed by homolytic rupture of O–O bond and formation of hydroxyl radicals (OH) (see Fig. 1). OH radicals are capable of degrading non-selectively and immediately organic molecules and decompose them into biodegradable compounds (Cheng et al. 2016; Gligorovski et al. 2015; Keen et al. 2014).

To confirm the formation of OH radicals during the reaction of CAA and H_2O_2, an excess of ethanol as OH radicals scavenger was added to the reaction mixture at different times. The results of Fig. 3 present the effect of addition of ethanol on the changes of the absorbance at 532 nm (λ_{max} of CAA in water, see Figure S1) with time during the chemical oxidation of CAA (1 mM) by H_2O_2 (1000 mM) under same operating conditions of pH, temperature, and stirring (initial pH = 3.0, T = 23–25 °C, stirring rate: 300 rpm). As it can be seen, the absorbance at 532 nm continuously decreased with time in the absence of ethanol to achieve almost complete decolorization after 300 min. However, the addition of ethanol to the mixture had a significant effect on the decrease in the absorbance at 532 nm. No change in the absorbance at 532 nm was observed when ethanol was added at the beginning of the reaction. The addition of ethanol after 60 min and 120 min stopped immediately the decay of the absorbance at 532 nm. These results confirmed the formation of OH radicals by reaction of CAA and H_2O_2 since ethanol is well known as powerful scavenger of OH radicals (Kozmér et al. 2016).

The changes of pH and conductivity during the chemical oxidation of CAA by H_2O_2 are given in Fig. 4a. A little increase in the pH from 3.0 to 3.4 was observed during 120 min of start of the experiment, and then it remained unchanged at 3.4 for the rest of the experiment. An increase in the conductivity from 6.18 to 6.47 mS/cm was observed after 90 min of the start of the reaction. This demonstrates that the chemical oxidation of CAA by H_2O_2 releases ionic species. Figure 4.b presents the results of analysis of chloride ions during the chemical oxidation of CAA by H_2O_2. As it can be seen, chloride ions concentration increased

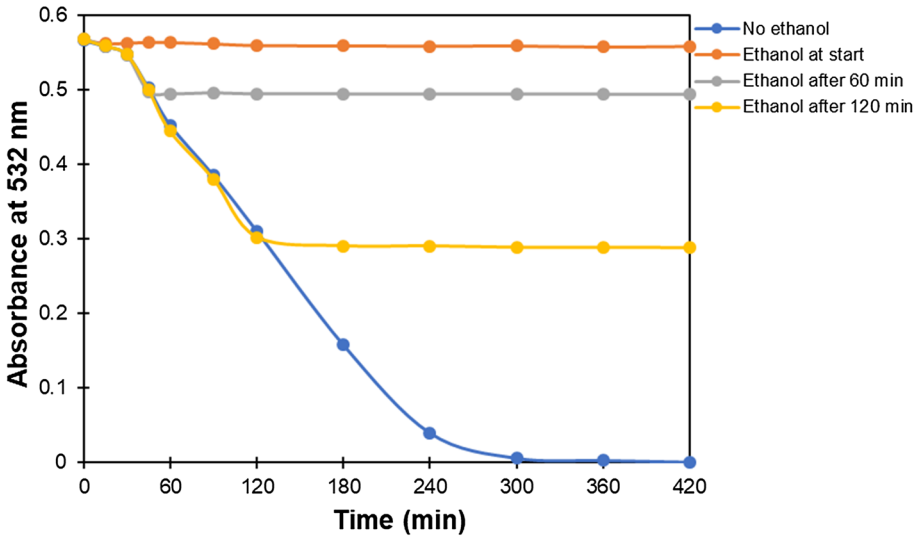

Fig. 3 Chemical oxidation of CAA by H_2O_2: Effect of addition of ethanol as OH radicals' scavenger. Operational conditions: initial CAA concentration: 209 mg/L (1 mM), H_2O_2 dose: 1000 mM, pH = 3.0, T = 23–25 °C, stirring rate: 300 rpm, ethanol: 20 Mm

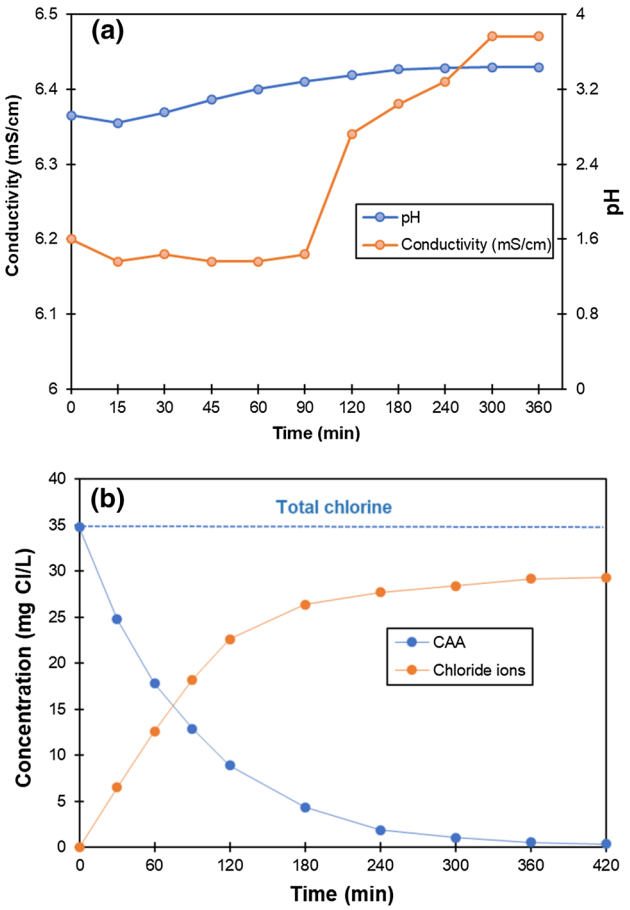

Fig. 4 Chemical oxidation of CAA by H_2O_2: **a** pH and conductivity, **b** CAA and chloride ion concentrations. Operational conditions: initial CAA concentration: 209 mg/L (1 mM), H_2O_2 dose: 1000 mM, initial pH = 3.0, T = 23–25 °C, stirring rate: 300 rpm

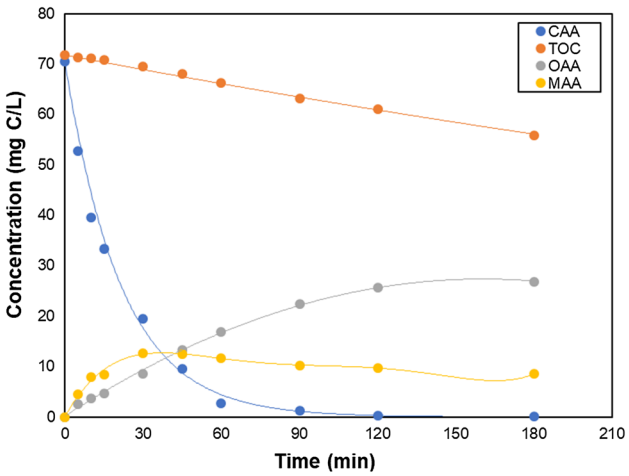

Fig. 5 Chemical oxidation of CAA by H_2O_2: CAA, TOC and carboxylic acids concentrations. Operational conditions: initial CAA concentration: 209 mg/L (1 mM), H_2O_2 dose: 1000 mM, initial pH = 3.0, T = 23–25 °C, stirring rate: 300 rpm

from the beginning of the experiment to reach a plateau at 29.2 mg Cl/L after 360 min. This result confirms the release of chloride ions during the chemical oxidation of CAA by H_2O_2 since the beginning of the reaction. The maximum of amount of chloride ions released was 84% of the total chlorine existing initially in the solution (no free chlorine was detected). This indicates that small portion of chlorine (16%) is still contained in chlorinated organic intermediates.

Figure 5 presents the changes of the concentrations of CAA, TOC, oxalic (OAA) and maleic (MAA) acids during the chemical oxidation of CAA (1 mM) by H_2O_2 (1000 mM) at initial pH 3.0 and room temperature. As can be observed, the decay in CAA concentration (in mg C/L) with time (pseudo-first-order rate constant of 0.012 min^{-1}) was about 30-fold more rapid than the removal of TOC

(pseudo-first-order rate constant of 0.0004 min^{-1}) during the chemical oxidation of CAA by H_2O_2. At the end of the experiment (420 min), almost complete depletion of CAA was achieved, while only 18% TOC was removed. The concentrations of OAA and MAA increased with time to reach plateaus after 420 min at 27.2 and 13.1 mg C/L, respectively. Considering mass balance, OAA and MAA represent 67% of TOC contained in the aqueous solution. This behavior reveals the formation of other unidentified intermediates. Meanwhile, the accumulation of carboxylic acids explains the slow decrease in TOC observed during the experiment. This might be due to the decrease in OH radicals' production with time, and the very slow chemical oxidation of carboxylic acid intermediates with H_2O_2.

Degradation of CAA by Fenton oxidation (H_2O_2/Fe^{2+})

In order to accelerate the mineralization of CAA aqueous solutions and achieve high TOC depletion yield, the effect of the addition of small amounts of iron(II) (Fe^{2+}) on the kinetics and efficiency of CAA degradation by H_2O_2/Fe^{2+} (Fenton oxidation) was evaluated. It was observed that the addition of Fe^{2+} to CAA aqueous solution changed the color of the solution from violet to dark brown indicating the formation of Fe^{2+}-CAA stable complex (see Figure S2). The stoichiometry of Fe^{2+}-CAA complex was determined by the method of continuous variations (also called Job's method) (Long and Pfeffer 2015; Renny et al. 2013). The theory behind the Job's method is that if the absorbance at a given wavelength of each solution is plotted against the mole fraction of the ligand, the maximum absorbance will occur at a mole fraction that corresponds to the composition. The illustration given in Figure S3 shows the continuous variations plot for the Fe^{2+}-CAA complex. As shown from the Job's method, Fe^{2+} and CAA form (1:2) complex, $Fe(CAA)_2^{2+}$.

Figure 6 presents the effect of H_2O_2 dose on the changes of CAA concentration with time during Fenton oxidation of 1 mM CAA aqueous solution using 0.5 mM Fe^{2+} (stoichiometric Fe^{2+} dose to form $Fe(CAA)_2^{2+}$) at pH 3.0 and room temperature under 300 rpm stirring. As shown in Fig. 6a, H_2O_2 dose affected the kinetics and efficiency Fenton oxidation of CAA. CAA depletion yields calculated after 60 min were 100, 99.9, 99.8, 96.1, 88.2, and 71.6% for 500, 200, 100, 75, 50, and 25 mM, respectively. Furthermore, as can be seen, CAA decay with time follows a pseudo-first-order kinetics for all H_2O_2 doses. Figure 6b shows a linear increase in pseudo-first-order rate constant (k_{obs}) with H_2O_2 dose between 25 to 100 mM, and then the slope decreases for higher H_2O_2 doses than 100 mM. The increase in H_2O_2 dose accelerates the production of HO radicals by Fenton reaction, which explains the improvement in CAA depletion yield and the increase in the rate constant with H_2O_2 dose. However, higher doses of H_2O_2 result in the deceleration of the rate constant with H_2O_2 dose due to speeding up the secondary reactions of H_2O_2 auto-decomposition and its reaction with OH radicals (Eqs. 6–7) (Bensalah et al. 2011; Ghatak 2014).

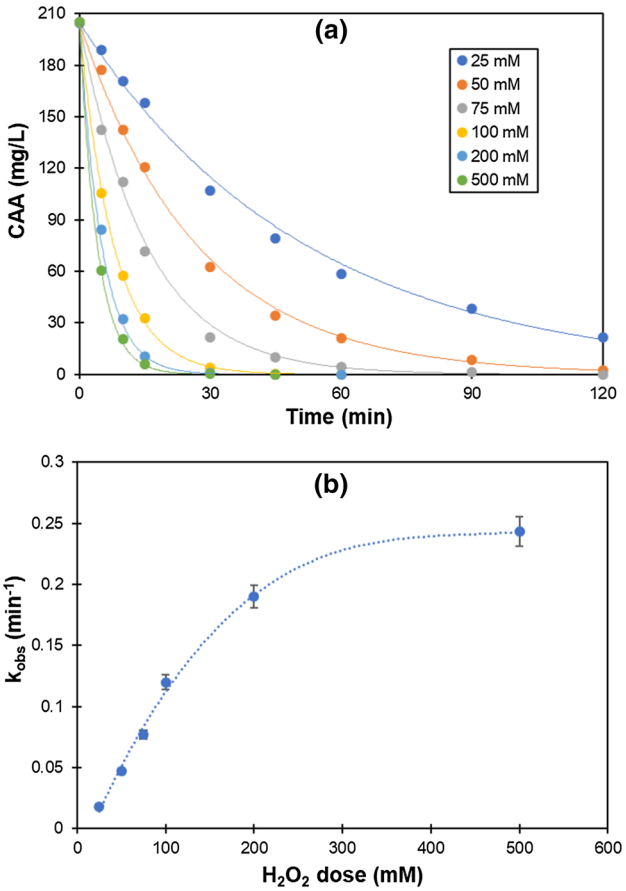

Fig. 6 Fenton oxidation of CAA in aqueous solutions: Effect of H_2O_2 dose on **a** CAA degradation, **b** Pseudo-first-order k_{obs}. Operational conditions: initial CAA concentration: 209 mg/L (1 mM), H_2O_2 dose: 25–500 mM, Fe^{2+} dose: 0.5 mM, initial pH = 3.0, T = 23–25 °C, stirring rate: 300 rpm

$$2H_2O_2 \rightarrow O_2 + 2H_2O \quad (6)$$

$$H_2O_2 + {}^{\cdot}OH \rightarrow HO_2^{\cdot} + H_2O \quad (7)$$

H_2O_2 dose of 100 mM is cost-effective and sufficient to achieve almost complete CAA decay within 60 min by Fenton oxidation. This optimal H_2O_2 dose is ten times lower than that required to achieve similar CAA depletion yield (1000 mM) during chemical oxidation of CAA by H_2O_2. This is due to the higher production of OH radicals by catalytic decomposition of H_2O_2 by Fe^{2+} (Fenton reaction, Eq. 1) than by chemical reaction between H_2O_2 and CAA.

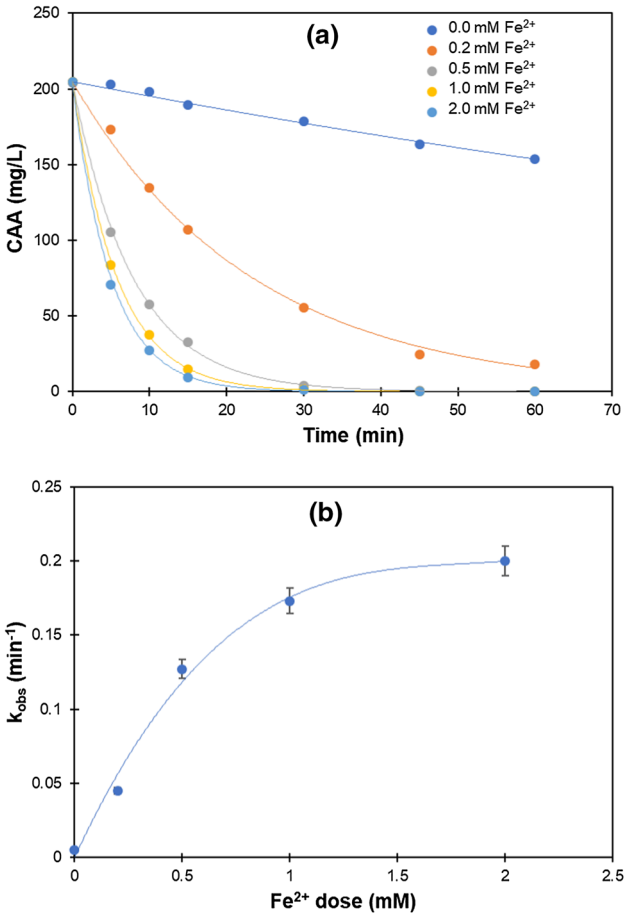

Fig. 7 Fenton oxidation of CAA in aqueous solutions: Effect of Fe^{2+} dose on: **a** CAA degradation, **b** Pseudo-first-order k_{obs}. Operational conditions: initial CAA concentration: 209 mg/L (1 mM), H_2O_2 dose: 100 mM, Fe^{2+} dose: 0.0–2.0 mM, initial pH = 3.0, T = 23–25 °C, stirring rate: 300 rpm

Figure 7 presents the changes of CAA concentration with time during Fenton oxidation of CAA (1 mM) using 100 mM H_2O_2 and different Fe^{2+} doses at pH 3.0 and room temperature under 300 rpm stirring. The increase in Fe^{2+} dose from 0.0 to 2 mM enhanced the kinetics and the yield of CAA depletion. These results confirmed that Fenton oxidation is more effective than chemical oxidation using H_2O_2. It is well documented (Babuponnusami and Muthukumar 2014; Pliego et al. 2015; Hui Zhang, et al. 2019; Oturan et al. 2012; Oliveira et al. 2014) that the presence of Fe^{2+} catalyzes the decomposition of H_2O_2 resulting in the formation of OH radicals (Eq. 1) that are capable of destroying organics in water. All the kinetic results shown in Fig. 6a can be modeled using a pseudo-first-order kinetics model. The pseudo-first-order rate constant, k_{obs}, increased linearly with the increase in Fe^{2+} dose from 0.0 up to 1.0 mM, with decreasing slope for Fe^{2+} doses higher than 1.0 mM (Fig. 7b). CAA depletion yields after 30 min were 12.6, 73.0, 96.1, 99.1, and 99.4% for Fe^{2+} doses of 0.0, 0.2, 0.5, 1.0, and 2.0 mM, respectively.

Table 1 Effect of initial pH on the degradation yield of some aromatic compounds by Fenton oxidation. Experimental conditions: initial pollutant concentration: 1 mM, H_2O_2 dose: 100 mM, Fe^{2+}: 1 mM, Time: 120 min, T = 23–25 °C, stirring: 300 rpm

Initial pH	$Degradation\ Yield(\%) = \frac{[X]_0 - [X]_{120}}{[X]_0} \times 100$ ($[X]_0$ and $[X]_{120}$ are concentrations of pollutant at time t = 0 min and t = 120 min)			
	CAA	Phenol	Benzoic Acid	Hydroquinone
3.0	100	100	100	100
4.0	99.4	82.7	85.2	93.1
5.0	92.2	71.5	77.3	83.6
6.0	81.6	58.2	65.4	73.8
7.0	58.1	38.2	43.5	55.1
8.0	44.6	20.1	32.6	37.2
9.0	33.8	11.4	16.8	21.6

Higher Fe^{2+} doses than 1 mM are not cost-effective since they did not significantly enhance the kinetics of the reaction. This indicates that a catalytic dose of Fe^{2+} (molar ratio (H_2O_2/Fe^{2+}) = 100) is required to achieve ≥ 99% CAA depletion within 30 min. It should be noted that generally smaller molar ratios (H_2O_2/Fe^{2+}) than 100 (between 1 and 50) have been reported in the literature (Mitsika et al. 2013; Biglarijoo et al. 2016). Using 1 mM Fe^{2+}, CAA/Fe^{2+} molar ratio is equal to 1, indicating that CAA ligand molecules were completely complexed with Fe^{2+} ions (considering a $Fe(CAA)_2^{2+}$ complex formula). Furthermore, it was found that, within the range 3.0 – 6.0, pH did not have a significant effect on CAA degradation and that Fe^{3+} and CAA form also stable complex $Fe(CAA)_2^{3+}$ (see Figure S4). These results show the importance of Fe^{2+}/Fe^{3+} organo-complexation in Fenton oxidation that might be related to the high solubility of $Fe(CAA)_2^{2+}$ complex enabling a rapid regeneration of the catalyst. In this case, CAA degradation by Fenton oxidation was less sensitive to pH due to the enhanced production of OH radicals by Fe^{2+}/Fe^{3+} organo-complexation. It should be noted that similar results have been reported related to the presence of organic ligands susceptible to form complexes with Fe^{2+}/Fe^{3+} ions (Messele et al. 2019). The results illustrated in Table 1 present the effect of initial pH on the degradation of some aromatic compounds including CAA, phenol, benzoic acid, and hydroquinone by Fenton oxidation. As it can be seen, Fenton oxidation achieved complete degradation of all aromatic compounds at pH 3.0 during 120 min. The initial pH affected the degradation yield of all compounds. Increasing pH to values higher than 3.0 decreased the pollutant degradation yield. It is markedly observed that CAA degradation was less affected by initial pH than the other compounds. More details about the effect of initial pH on CAA degradation by Fenton oxidation are given in Figure S5.

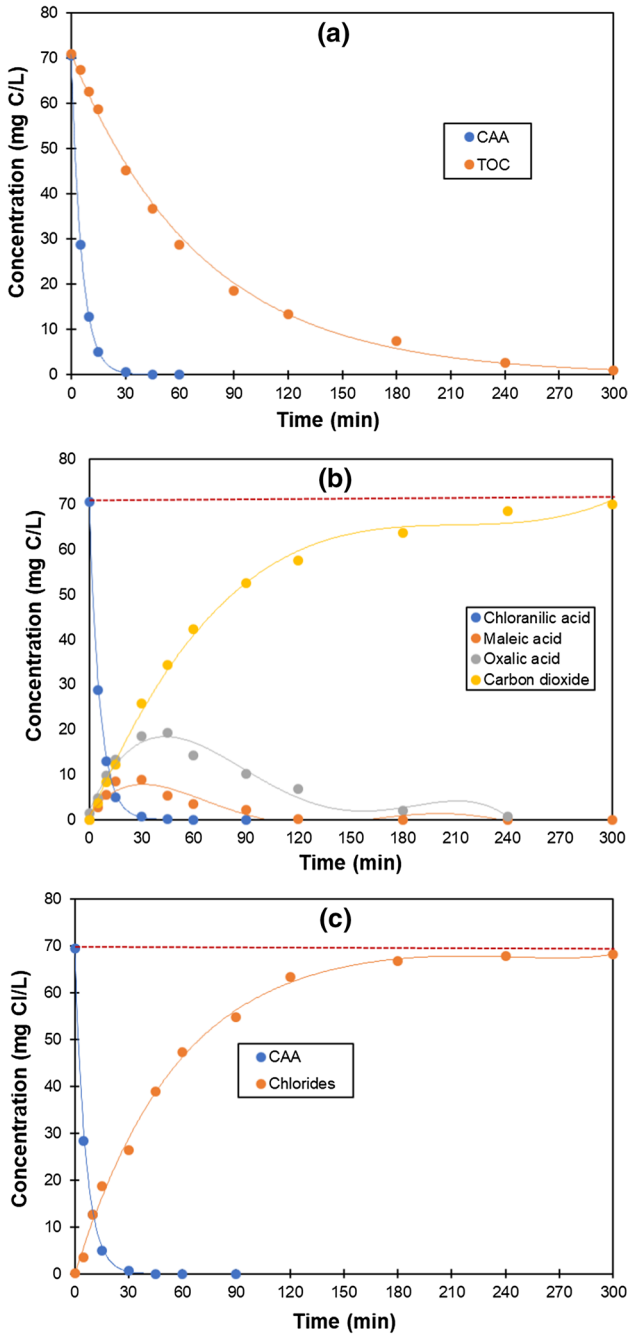

Fig. 8 Fenton oxidation of CAA: **a** CAA, TOC, and intermediates concentrations; **b** CAA, Carboxylic intermediates, and carbon dioxide concentrations; **c** CAA and chloride ions. Operational conditions: initial CAA concentration: 209 mg/L (1 mM), H_2O_2 dose: 100 mM, Fe^{2+}: 1 mM, initial pH = 3.0, T = 23–25 °C, stirring rate: 300 rpm

Figure 8 presents the results of CAA mineralization during Fenton oxidation of 1 mM CAA aqueous solution using 100 mM H_2O_2 and 1 mM Fe^{2+} at pH 3.0 and room temperature. As shown in Fig. 8a, CAA decay was too much more rapid than TOC depletion with pseudo-first-order rate constants of 0.173 and 0.014 min^{-1}, respectively. CAA was completely depleted after 60 min; while 99% TOC was depleted after 300 min (see Fig. 8a). CAA decay was accompanied with a simultaneous formation of chloride ions, CO_2, OAA, and MAA from the beginning of photochemical treatment (Fig. 8b). It was found that 98% of organic chlorine was converted into chloride ions by Fenton oxidation after 300 min. No chlorate and perchlorate ions were detected, but small amount of free chlorine was formed based on N,N-diethyl-p-phenylenediamine (DPD) rapid test (Rice et al. 2017). These results indicate that chloride ions and carbon dioxide are the major final products of CAA degradation using Fenton oxidation. OAA and MAA were formed as intermediate species that were converted into CO_2 and they were mostly depleted at the end of the treatment. These results reveal that the mechanism of CAA degradation by Fenton oxidation could involve similar steps than chemical oxidation using H_2O_2. During Fenton oxidation, both Fenton reaction and nucleophilic substitution of Cl with OOH followed by homolytic rupture of O – O bond produce more important amounts of hydroxyl radicals, which enhances CAA mineralization. It is remarkable that no accumulation of carboxylic acids was observed during CAA degradation by Fenton oxidation. This result confirms the importance of $Fe^{2+/3+}$-CAA complex formation that enables high solubility for iron(II)/iron(III) catalyst and accelerates the regeneration of Fe^{2+} catalyst, and thus large production of OH radicals occurs.

Table 2 Optimization of experimental parameters on the discoloration yield of MB by H_2O_2-based chemical methods. Experimental conditions: MB: 0.0125 mM (4 mg/L), pH = 3.0, T = 23–25 °C, Stirring rate: 300 rpm, Time: 120 min. $\boldsymbol{Discoloration\ Yield}(\%) = \frac{Abs_0 - Abs_{120}}{Abs_0} \times 100$ (Abs_0 and Abs_{120} are absorbance at 664 nm at time t = 0 min and t = 120 min)

H_2O_2 (mM)	CAA (mM)	Fe^{2+} (mM)	*Discoloration yield*(%)
20	0	0	5.8
25	0	0	10.8
30	0	0	11.2
25	0.010	0	27.3
25	0.025	0	58.0
25	0.050	0	59.1
25	0	0.010	64.8
25	0	0.025	97.1
25	0	0.050	96.9
25	0.025	0.010	97.8
25	0.025	0.025	99.9
25	0.025	0.050	96.7

Decolorization of MB aqueous solution by H_2O_2/CAA, H_2O_2/Fe^{2+}, and H_2O_2/CAA/Fe^{2+}

The concentrations of reagents used to decolorize 0.025 mM MB solutions at pH = 3.0 and T = 23–25 °C

under stirring rate of 300 rpm were optimized in preliminary experiments (see Table 2). The results of Table 2 demonstrate that the optimal conditions to reach the maximum discoloration yields were: 25 mM H_2O_2, 0.025 mM Fe^{2+}, and 0.025 mM CAA. Figure 9 presents the changes of the normalized absorbance (Abs_t/Abs_0) (with Abs_t and Abs_0 are the absorbencies of MB at 664 at an instant t and at t = 0 s) of MB aqueous solutions with time during the degradation of MB (0.0125 mM) aqueous solution using different H_2O_2-based chemical oxidation methods (see Figure S6 for color differences). As it can be seen, $H_2O_2/CAA/Fe^{2+}$ was the most effective oxidation method to remove MB from water. Fenton oxidation (H_2O_2/Fe^{2+}) was more efficient than H_2O_2/CAA (Figure S7 shows the changes of UV–visible spectra with time for the different H_2O_2-based chemical oxidation methods). The chemical oxidation with H_2O_2 alone was the lowest effective method. The complete decolorization of MB aqueous solution was achieved after 75 min with $H_2O_2/CAA/Fe^{2+}$, while at this time, decolorization percent were 7.5, 42.0, and 90.6% for H_2O_2 alone, H_2O_2/CAA, and H_2O_2/Fe^{2+}, respectively. The rate constant calculated from the fitted data to pseudo-first-order kinetics model was 0.069, 0.031, 0.007, and 0.0007 min^{-1} for $H_2O_2/CAA/Fe^{2+}$, H_2O_2/Fe^{2+}, H_2O_2/CAA, and H_2O_2 alone, respectively. Coupling H_2O_2 with CAA was able to partially decolorize the MB solution due to the small amount of OH radicals formed from the chemical oxidation of CAA by H_2O_2. H_2O_2/Fe^{2+} (Fenton's reagent) was more effective than H_2O_2/CAA due to larger amount of OH radicals produced by Fenton reaction. The cost of each process can be estimated based on the prices of chemicals. Considering that the same chemicals are used, it is obvious that $H_2O_2/CAA/Fe^{2+}$ is the most cost-effective compared to the other processes. Figure 10 shows the effect of initial pH on the changes of the normalized absorbance (Abs_t/Abs_0) with time during MB decolorization using $H_2O_2/CAA/Fe^{2+}$. As it can be seen, the increase in pH from 3.0 to 6.0 did not have a significant effect on the kinetics of MB decolorization; however, higher initial pH than 6.0 decelerated the MB decolorization. MB decolorization yield calculated after 60 min was 98.9, 98.4, 97.6, 95.4, 75.5, 49.3, and 32.6 for pH 3.0, 4.0, 5.0, 6.0, 7.0, 8.0, and 9.0, respectively. CAA can also form stable complexes with Fe^{2+}/Fe^{3+} that increases the solubility of Fe^{3+} and then keep similar amount of catalyst available to decompose H_2O_2. The results of Fig. 10 confirm this hypothesis since the initial pH in the range 3.0 – 6.0 did not affect the MB decolorization by $H_2O_2/CAA/Fe^{2+}$ system.

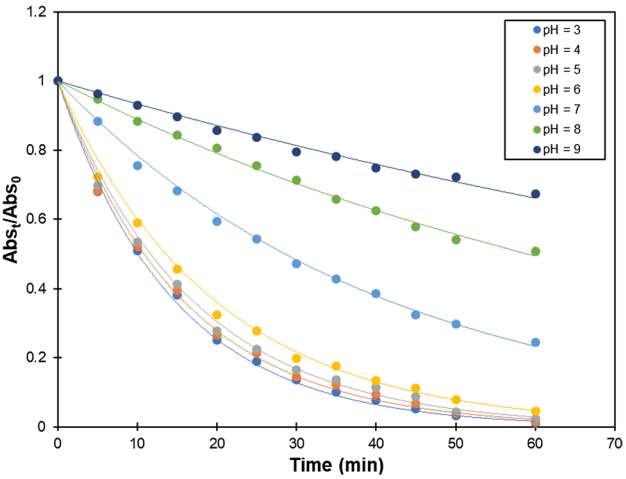

Fig. 10 Effect of initial pH on the decolorization of MB aqueous solution using different $H_2O_2/CAA/Fe^{2+}$ system. Experimental conditions: MB: 0.0125 mM (4 mg/L), H_2O_2: 25 mM, Fe^{2+}: 0.025 mM, CAA: 0.025 mM, pH = 3.0–9.0, T = 23–25 °C, stirring: 300 rpm

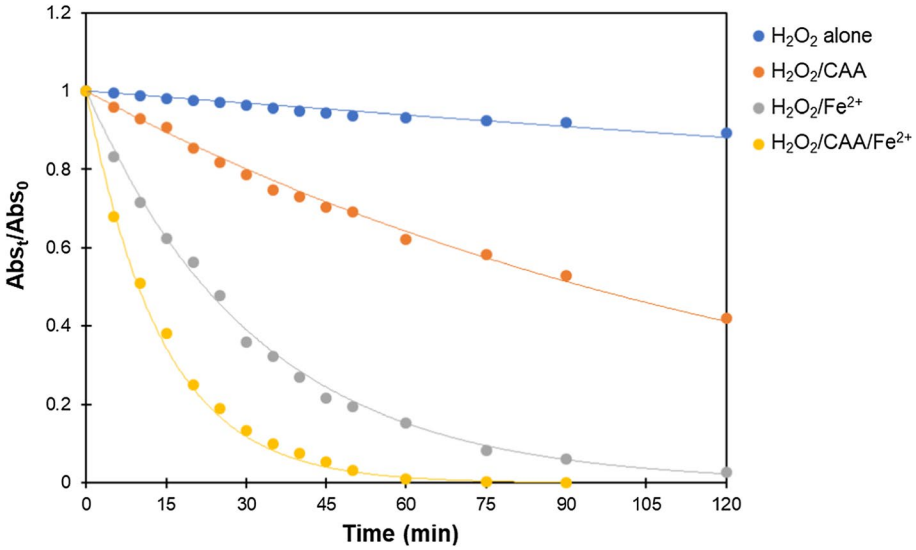

Fig. 9 Decolorization of MB aqueous solutions using different H_2O_2-based chemical oxidation methods. Operational conditions: MB: 0.0125 mM (4 mg/L), H_2O_2: 25 mM, Fe^{2+}: 0.025 mM, CAA: 0.025 mM, pH = 3.0, *T* = 23–25 °C, stirring rate: 300 rpm

Table 3 Estimated costs of H_2O_2-based methods for MB discoloration. Experimental conditions: MB: 0.0125 mM (4 mg/L), H_2O_2: 25 mM, Fe^{2+}: 0.025 mM, CAA: 0.025 mM, pH = 3.0, T = 23–25 °C, stirring rate: 300 rpm

Treatment method	Chemical costs ($/m^3)	Post-treatment costs ($/m^3)	Total costs ($/m^3)
H_2O_2/CAA	0.35	0.40	0.75
H_2O_2/Fe^{2+}	0.25	0.55	0.80
H_2O_2/CAA/Fe^{2+}	0.40	0.20	0.60

The higher effectiveness of H_2O_2/CAA/Fe^{2+} in decolorizing MB aqueous solution is due to the acceleration of iron(II) catalyst regeneration in Fenton oxidation mechanism. CAA (quinonoid substance) is capable of reducing Fe^{3+} into Fe^{2+} (Taran 2017; Sander et al. 2015) and then continuously feeds up the system with OH radicals. The estimated costs (($/m^3) calculated based on the chemicals cost (using technical grade chemicals) and the post-treatment costs (filtration, washing, and AC adsorption) are illustrated in Table 3. H_2O_2/CAA/Fe^{2+} costs are less than H_2O_2/Fe^{2+} and H_2O_2/CAA processes. H_2O_2/CAA/Fe^{2+} is the most cost-effective process due to cheaper post-treatment (AC adsorption).

Conclusion

CAA can be slowly degraded by chemical oxidation with H_2O_2. The reaction required high amount of H_2O_2 (H_2O_2/CAA molar ratio = 1000) to achieve the almost complete removal of CAA within 420 min. The addition of ethanol (as OH radicals scavenger) confirmed the production of OH radicals. TOC analysis and chromatography results indicated that low organic carbon mineralization yield was achieved with accumulation of carboxylic acids intermediates and the release of 84% organic chlorine. The addition of Fe^{2+} enhanced CAA degradation and reduced the amount of H_2O_2 required to achieve complete CAA decay and 99% TOC removal. It seems that the formation of $Fe^{2+/3+}$-CAA complexes enables accelerates the regeneration of Fe^{2+} catalyst, and thus large production of OH radicals occurs. Furthermore, H_2O_2/CAA/Fe^{2+} system was more effective in decolorizing MB aqueous solution than H_2O_2/CAA and H_2O_2/Fe^{2+} systems. This might be due to larger OH radicals' production and more rapid Fe^{2+} regeneration. This indicates that the addition of small amount of CAA (quinonoid compound) could be a promising method to enhance the effectiveness of Fenton oxidation without significant rise in costs compared to coupling Fenton oxidation with photolysis, sonolysis, or electrolysis.

Supplementary Information The online version contains supplementary material available at https://doi.org/10.1007/s13762-021-03822-0.

Acknowledgements Authors acknowledge the Central Laboratories Unit at Qatar University for helping in performing the analysis of water samples.

Funding Open Access funding is provided by the Qatar National Library (QNL).

Conflict of interest The authors declare that they have no conflict of interest.

Open Access This article is licensed under a Creative Commons Attribution 4.0 International License, which permits use, sharing, adaptation, distribution and reproduction in any medium or format, as long as you give appropriate credit to the original author(s) and the source, provide a link to the Creative Commons licence, and indicate if changes were made. The images or other third party material in this article are included in the article's Creative Commons licence, unless indicated otherwise in a credit line to the material. If material is not included in the article's Creative Commons licence and your intended use is not permitted by statutory regulation or exceeds the permitted use, you will need to obtain permission directly from the copyright holder. To view a copy of this licence, visit http://creativecommons.org/licenses/by/4.0/.

References

Ameta R, Chohadia AK, Jain A, Punjabi PB (2018) Fenton and photo-fenton processes, in advance oxidation processes for waste water treatment. Emerg Green Chem Technol. https://doi.org/10.1016/B978-0-12-810499-6.00003-6

Babuponnusami A, Muthukumar K (2014) A review on Fenton and improvements to the Fenton process for wastewater treatment. J Environ Chem Eng. https://doi.org/10.1016/j.jece.2013.10.011

Bensalah N, Khodary A, Abdel-Wahab A (2011) Kinetic and mechanistic investigations of mesotrione degradation in aqueous medium by Fenton process. J Hazard Mater. https://doi.org/10.1016/j.jhazmat.2011.02.060

Biglarijoo N, Mirbagheri SA, Ehteshami M, Ghaznavi SM (2016) Optimization of Fenton process using response surface methodology and analytic hierarchy process for landfill leachate treatment. Process Saf Environ Prot. https://doi.org/10.1016/j.psep.2016.08.019

Boonrattanakij N, Lu MC, Anotai J (2011) Iron crystallization in a fluidized-bed Fenton process. Water Res. https://doi.org/10.1016/j.watres.2011.03.045

Buxton GV, Greenstock CL, Helman WP, Ross AB (1988) Critical Review of rate constants for reactions of hydrated electrons, hydrogen atoms and hydroxyl radicals (·OH/·O− in Aqueous Solution. J Phys Chem Ref Data. https://doi.org/10.1063/1.555805

Chen L, Ma J, Li X, Zhang J, Fang J, Guan Y, Xie P (2011) Strong enhancement on Fenton oxidation by addition of hydroxylamine to accelerate the ferric and ferrous iron cycles. Environ Sci Technol. https://doi.org/10.1021/es2002748

Chen R, Pignatello JJ (1997) Role of quinone intermediates as electron shuttles in fenton and photoassisted fenton oxidations of aromatic compounds. Environ Sci Technol. https://doi.org/10.1021/es9610646

Cheng M, Zeng G, Huang D, Lai C, Xu P, Zhang C, Liu Y (2016) Hydroxyl radicals based advanced oxidation processes (AOPs) for remediation of soils contaminated with organic compounds: a review. Chem Eng J. https://doi.org/10.1016/j.cej.2015.09.001

Clarizia L, Russo D, Di Somma I, Marotta R, Andreozzi R (2017) Homogeneous photo-Fenton processes at near neutral pH: A review. Appl Catal B Environ. https://doi.org/10.1016/j.apcatb.2017.03.011

Duesterberg CK, Mylon SE, Waite TD (2008) pH effects on iron-catalyzed oxidation using Fenton's reagent. Environ Sci Technol. https://doi.org/10.1021/es801720d

Duesterberg CK, Waite TD (2007) Kinetic modeling of the oxidation of p-hydroxybenzoic acid by Fenton's reagent: Implications of the role of quinones in the redox cycling of iron. Environ Sci Technol. https://doi.org/10.1021/es0628699

Ganiyu SO, Zhou M, Martínez-Huitle CA (2018) Heterogeneous electro-Fenton and photoelectro-Fenton processes: A critical review of fundamental principles and application for water/wastewater treatment. Appl Catal B Environ. https://doi.org/10.1016/j.apcatb.2018.04.044

García O, Isarain-Chávez E, Garcia-Segura S, Brillas E, Peralta-Hernández JM (2013) Degradation of 2,4-dichlorophenoxyacetic acid by electro-oxidation and electro-Fenton/BDD processes using a pre-pilot plant. Electrocatalysis. https://doi.org/10.1007/s12678-013-0135-4

Ghatak HR (2014) Advanced oxidation processes for the treatment of biorecalcitrant organics in wastewater. Crit Rev Environ Sci Technol. https://doi.org/10.1080/10643389.2013.763581

Giraldo-Aguirre AL, Serna-Galvis EA, Erazo-Erazo ED, Silva-Agredo J, Giraldo-Ospina H, Flórez-Acosta OA, Torres-Palma RA (2018) Removal of β-lactam antibiotics from pharmaceutical wastewaters using photo-Fenton process at near-neutral pH. Environ Sci Pollut Res. https://doi.org/10.1007/s11356-017-8420-z

Gligorovski S, Strekowski R, Barbati S, Vione D (2015) Environmental Implications of Hydroxyl Radicals (•OH). Chem Rev. https://doi.org/10.1021/cr500310b

Jeong J, Song W, Cooper WJ, Jung J, Greaves J (2010) Degradation of tetracycline antibiotics: mechanisms and kinetic studies for advanced oxidation/reduction processes. Chemosphere. https://doi.org/10.1016/j.chemosphere.2009.11.024

Keen OS, McKay G, Mezyk SP, Linden KG, Rosario-Ortiz FL (2014) Identifying the factors that influence the reactivity of effluent organic matter with hydroxyl radicals. Water Res. https://doi.org/10.1016/j.watres.2013.10.049

Kozmér Z, Takács E, Wojnárovits L, Alapi T, Hernádi K, Dombi A (2016) The influence of radical transfer and scavenger materials in various concentrations on the gamma radiolysis of phenol. Radiat Phys Chem. https://doi.org/10.1016/j.radphyschem.2015.12.011

Li J, Wan Y, Li Y, Yao G, Lai B (2019) Surface Fe(III)/Fe(II) cycle promoted the degradation of atrazine by peroxymonosulfate activation in the presence of hydroxylamine. Appl Catal B Environ. https://doi.org/10.1016/j.apcatb.2019.117782

Li P, Wang W, Sun Q, Li Z, Du A, Bi S, Zhao Y (2013) Insights into the mechanism of the reaction between tetrachloro-p- benzoquinone and hydrogen peroxide and their implications in the catalytic role of water molecules in producing the hydroxyl radial. ChemPhysChem. https://doi.org/10.1002/cphc.201300395

Liu X, Zhou Y, Zhang J, Luo L, Yang Y, Huang H, Peng H, Tang L, Mu Y (2018) Insight into electro-Fenton and photo-Fenton for the degradation of antibiotics: Mechanism study and research gaps. Chem Eng J. https://doi.org/10.1016/j.cej.2018.04.142

Long BM, Pfeffer FM (2015) On the use of shortcuts in the method of continuous variation (Job's method). Supramol Chem. https://doi.org/10.1080/10610278.2014.909044

Martínez-Costa JI, Rivera-Utrilla J, Leyva-Ramos R, Sánchez-Polo M, Velo-Gala I, Mota AJ (2018) Individual and simultaneous degradation of the antibiotics sulfamethoxazole and trimethoprim in aqueous solutions by Fenton, Fenton-like and photo-Fenton processes using solar and UV radiations. J Photochem Photobiol A Chem. https://doi.org/10.1016/j.jphotochem.2018.04.014

Martínez-Huitle CA, Quiroz MA, Comninellis C, Ferro S, De Battisti A (2004) Electrochemical incineration of chloranilic acid using Ti/IrO2, Pb/PbO2 and Si/BDD electrodes. Electrochim Acta. https://doi.org/10.1016/j.electacta.2004.07.035

Messele SA, Bengoa C, Stüber FE, Giralt J, Fortuny A, Fabregat A, Font J (2019) Enhanced degradation of phenol by a fenton-like system (Fe/EDTA/h2 o2) at circumneutral pH. Catalysts. https://doi.org/10.3390/catal9050474

Mitsika EE, Christophoridis C, Fytianos K (2013) Fenton and Fenton-like oxidation of pesticide acetamiprid in water samples: Kinetic study of the degradation and optimization using response surface methodology. Chemosphere. https://doi.org/10.1016/j.chemosphere.2013.06.033

Nidheesh PV (2015) Heterogeneous Fenton catalysts for the abatement of organic pollutants from aqueous solution: a review. RSC Adv. https://doi.org/10.1039/c5ra02023a

Nidheesh PV, Gandhimathi R, Ramesh ST (2013) Degradation of dyes from aqueous solution by Fenton processes: a review. Environ Sci Pollut Res. https://doi.org/10.1007/s11356-012-1385-z

Oliveira C, Alves A, Madeira LM (2014) Treatment of water networks (waters and deposits) contaminated with chlorfenvinphos by oxidation with Fenton's reagent. Chem Eng J. https://doi.org/10.1016/j.cej.2013.12.026

Oturan N, Brillas E, Oturan MA (2012) Unprecedented total mineralization of atrazine and cyanuric acid by anodic oxidation and electro-Fenton with a boron-doped diamond anode. Environ Chem Lett. https://doi.org/10.1007/s10311-011-0337-z

Pliego G, Zazo JA, Garcia-Muñoz P, Munoz M, Casas JA, Rodriguez JJ (2015) Trends in the Intensification of the fenton process for wastewater treatment: an overview. Crit Rev Environ Sci Technol. https://doi.org/10.1080/10643389.2015.1025646

Qiang Z, Chang JH, Huang CP (2003) Electrochemical regeneration of Fe2+ in Fenton oxidation processes. Water Res. https://doi.org/10.1016/S0043-1354(02)00461-X

Rahim Pouran S, Abdul Raman AA, Wan Daud WMA (2014) Review on the application of modified iron oxides as heterogeneous catalysts in Fenton reactions. J Clean Prod. https://doi.org/10.1016/j.jclepro.2013.09.013

Renny JS, Tomasevich LL, Tallmadge EH, Collum DB (2013) Method of continuous variations: Applications of job plots to the study of molecular associations in organometallic chemistry. Angew Chemie - Int Ed. https://doi.org/10.1002/anie.201304157

Rice EW, Baird RB, Eaton AD (2017) 4500-Cl Chlorine (Residual). Stand Methods Exam Water Wastewater. https://doi.org/10.2105/SMWW.2882.078

Sander M, Hofstetter TB, Gorski CA (2015) Electrochemical analyses of redox-active iron minerals: A review of nonmediated and mediated approaches. Environ Sci Technol. https://doi.org/10.1021/acs.est.5b00006

Taran O (2017) Electron transfer between electrically conductive minerals and quinones. Front Chem. https://doi.org/10.3389/fchem.2017.00049

Telles C, Granhen Tavares CR, (2012) Fenton´s process for the treatment of mixed waste chemicals, In: Organic Pollutant Ten Years After Stock. Conv Environ Anal Updat. https://doi.org/10.5772/31225

Thomas M, Białecka B, Zdebik D (2017) Removal of organic compounds from wastewater originating from the production of printed circuit boards by UV-Fenton method. Arch Environ Prot. https://doi.org/10.1515/aep-2017-0044

Thomas M, Zdebik D (2019) Treatment of real textile wastewater by using potassium ferrate(VI) and fe(III)/H2O2 application of aliivibrio fischeri and brachionus plicatilis tests for toxicity assessment. Fibres Text East Eur. https://doi.org/10.5604/01.3001.0013.0746

Treviño-Quintanilla LG, Freyre-González JA, Guillén-Garcés RA, Olvera C (2011) Molecular characterization of chloranilic acid degradation in Pseudomonas putida TQ07. J Microbiol. https://doi.org/10.1007/s12275-011-1507-1

Verma V, Chaudhari PK (2020) Optimization of multiple parameters for treatment of coking wastewater using Fenton oxidation. Arab J Chem. https://doi.org/10.1016/j.arabjc.2020.02.008

Wang W, Moe B, Li J, Qian Y, Zheng Q, Li XF (2016) Analytical characterization, occurrence, transformation, and removal of the emerging disinfection byproducts halobenzoquinones in water. TrAC - Trends Anal Chem. https://doi.org/10.1016/j.trac.2016.03.004

Wang W, Qian Y, Li J, Moe B, Huang R, Zhang H, Hrudey SE, Li XF (2014) Analytical and toxicity characterization of halo-hydroxylbenzoquinones as stable halobenzoquinone disinfection byproducts in treated water. Anal Chem. https://doi.org/10.1021/ac5007238

Yue H, Wang S, Yang Z, Li Q, Lin S, He D (2015) Ultra-thick porous films of graphene-encapsulated silicon nanoparticles as flexible anodes for lithium ion batteries. Electrochim Acta. https://doi.org/10.1016/j.electacta.2015.06.042

Zhang M-H, Dong H, Zhao L, Wang D-x, Meng Di (2019) A review on Fenton process for organic wastewater treatment based on optimization perspective. Sci Total Environ. https://doi.org/10.1016/j.scitotenv.2019.03.180

Zhu B-Z, Fan R-M, Qu N (2012) A novel mechanism for metal-independent hydroxyl radical production by hydrogen peroxide and halogenated quinones. Mini Rev Org Chem. https://doi.org/10.2174/157019311797440290

Zhu BZ, Kalyanaraman B, Bin Jiang G (2007) Molecular mechanism for metal-independent production of hydroxyl radicals by hydrogen peroxide and halogenated quinones. Proc Natl Acad Sci. https://doi.org/10.1073/pnas.0704030104

Zhu BZ, Zhao HT, Kalyanaraman B, Frei B (2002) Metal-independent production of hydroxyl radicals by halogenated quinones and hydrogen peroxide: an ESR spin trapping study. Free Radic Biol Med. https://doi.org/10.1016/S0891-5849(01)00824-3

Zhu BZ, Zhu JG, Mao L, Kalyanaraman B, Shan GQ (2010) Detoxifying carcinogenic polyhalogenated quinones by hydroxamic acids via an unusual double Lossen rearrangement mechanism. Proc Natl Acad Sci U S A. https://doi.org/10.1073/pnas.1010950107